DOI: https://doi.org/10.61762/pajevol9iss2art006

PLATFORM - A Journal of Engineering

Received: 20 August 2024, Revised: 13 June 2025, Accepted: 27 June 2025, Published: 30 June 2025, Publisher: UTP Press, Creative Commons: CC BY 4.0

PHYSICAL AND MECHANICAL PROPERTIES OF POWDER INJECTION MOULDED 316L STAINLESS STEEL TITANIUM-COPPER ALLOY

Lucas Lim Sheng Onn, Faiz Ahmad*, Saad Ali

Department of Mechanical Engineering, University Teknologi PETRONAS, Malaysia

*E-mail: faizahmad@utp.edu.my

ABSTRACT

316L-Ti-Cu alloy was developed with two variations of copper at 1 vol% and 3 vol% through powder injection moulding to investigate the influence of copper on the alloy. This alloy has not been researched before and is expected to serve as an alternative for implants that possess beneficial antibacterial effects from copper, which can mitigate infection-related issues that occur during orthopaedic surgery. Two sintering environments will be conducted which are under vacuum and under argon-5% hydrogen, to ascertain the optimal properties of the alloy. The main reason behind the different sintering atmospheres is to prevent the oxidation of copper, which easily forms under a small presence of oxygen, and it can affect the particle bonding during the sintering process, which subsequently affects the characteristics of the alloy. The maximum sintered density obtained was 89.9% from the 1 vol% Cu sample sintered under a vacuum atmosphere, indicating high porosity in all the samples. The scanning electron microscope (SEM) and energy dispersive x-ray spectroscopy (EDS) analysis on the samples indicate that high amounts of pores were observed, along with the formation of oxides and carbides, which explains the low density and mechanical properties obtained. From the tensile test, the 1 vol% Cu sample sintered under vacuum yields the highest Young's modulus at 35.2 GPa, whereas the lowest Young's modulus of 11.01 GPa was obtained for 3 vol% Cu sintered under argon-hydrogen. All samples possess Young' modulus which are similar to those of trabecular and cortical bone. With such properties shown and the antibacterial properties of copper added into the alloy, the potential of this alloy for orthopaedic implant applications is solidified. The future work of this research would be focusing on the optimisation of the properties of the alloy.

Keywords: *Implant material, tensile strength, microhardness, antibacterial properties, vacuum sintering, argon-hydrogen sintering, oxidation*

INTRODUCTION

The rate of bioimplant surgery involving various bone-related injuries and diseases has witnessed a significant increase over the last few years, and the key contributing factors to this concerning issue are due to an increase in chronic diseases and lifestyle disorders [1]-[2]. This situation has led to a significant increase in the area of research and development related to the materials for implant applications. Due to the fact that the human body comprises a highly complex biological system, it is extremely sensitive to any foreign material as it has the potential to cause life-threatening side effects such as tumours, corroded elements flowing through the bloodstream and damage to the tissues found in the human body [3]. Therefore, it is vital that the material selected for the implant has excellent compatibility with human tissues and bodily fluids and does not negatively impact human anatomy [1],[3].

The primary function of an implant is to provide assistance in ensuring that the patient's damaged part is able to function properly [3]-[4]. Hence, the material to be used for implant purposes must meet the main criteria to ensure that the implant can cope with its working conditions and environment. The types of material used in implant applications over the past few years consist of 316L Stainless Steel-HA, Ti–6Al,

4V-HA and 316L-Titanium. Each has its strengths and weaknesses. Titanium alloy is more vulnerable to wear where articulation is needed, as it is softer compared to its other metallic counterparts [5]. Meanwhile for 316L Stainless Steel, due to its high elastic modulus, it is highly vulnerable to stress shielding which is the lack of balance of stress due to the dissimilarity in mechanical properties between the implant and bone, which can potentially lead to treatment failure which is common in most metallic implant [5]-[6].

However, one common trend observed from these materials is the lack of antibacterial properties, which is crucial in ensuring that any form of infection does not occur. This is highly critical as it will heavily hamper the healing process when the infection occurs, leading the patient to undertake long-term antibiotic treatment or even a secondary operation to remove the implant [7]. This is because it is very difficult to provide treatment to infections in bone sites due to their deep localisation in the tissue and the microorganism involved [8]. According to Jin et al. [9], copper is widely known as an important element in the human body and for having strong antibacterial and antifungal effects. These findings are also aligned with those of Jacobs et al. [8], whereby it was mentioned that copper exhibits antibacterial abilities that are able to aid in angiogenic ability and osteogenesis. Therefore, this explains the rise in research related to copper in implant applications.

Despite the improvement and further development made over the last few years, there is still a limitation in the properties of the material that needs to be addressed to ensure that the implant does not have stress shielding effects, but most importantly, that the possibility of infections is eliminated, as it can jeopardise the healing process. The challenge, therefore, is to develop a material that possesses excellent mechanical properties and compatibility with antibacterial functions compared to its counterpart. The motivation behind this research is aligned with that mentioned by Gobbi et al. [10], which is to develop a material with high longevity and exceptional biocompatibility for implant application. Therefore, it is proposed that the development of 316L-Ti-Cu alloy be initiated and its properties analysed due to its highly expected properties for bioimplant applications that other materials do not possess. Moreover, an implant containing copper can further enhance the recovery process of blood supply for the damaged tissues, which improves the overall adaptation of materials [9]. That said, this material is highly anticipated to possess great mechanical and physical properties and great biocompatibility with the human body, which is suitable for bioimplant applications.

This study investigates the influence of copper alloying, i.e., 1 vol.% and 3 vol.%, on the sintering behaviour and properties of a novel 316L-Ti-Cu alloy fabricated via powder injection moulding (PIM). Two atmospheres, vacuum and argon-5% hydrogen, were used during sintering to prevent copper oxidation and its detrimental effects on atomic diffusion during sintering and mechanical properties. After fabrication, the sintered composites were characterised for morphology and grain structure using scanning electron microscope (SEM) and energy dispersive x-ray spectroscopy (EDS) elemental distribution. Furthermore, the densification was quantified through sintered density measurement. Mechanical properties, including microhardness and tensile strength, were measured for all the samples. The study further suggests biocompatibility tests for the presented sample formulations in future studies.

METHODOLOGY

Gas atomised copper powder had a D90 of 22 µm and 99% purity from GoodFellow Cambridge Ltd., UK. Spherical shape gas-atomised 316L SS (Alfa Aesar, UK) and irregularly shaped Ti powder (Alfa Aesar, UK) with particle sizes D90 < 32 µm. A Hitachi TM3000 SEM was used to determine the morphology of metallic powders.

Two different formulations were prepared with 1 and 3 vol.% Cu, with 3 vol.% Ti in both formulations, and the remaining would be 316L Stainless steel. The powder loading is set at 65 vol.% for each feedstock, with the remaining 35 vol.% being the binders. The fabrication begins with mixing the 316L Stainless steel powder with the titanium and copper using a turbular mixer for a duration of 1 hour. Next, the mixed powders and the binders, which consist of 70 vol.% paraffin wax, 25 vol.% of polypropylene, and 5 vol.% of stearic acid, are mixed in a Z-blade mixer for 1 hour at 11 rpm and with a temperature of 160°C to form the feedstock. Next, the vertical injection moulding machine will

manufacture the green part under conditions set at 5 bars of pressure, a temperature of 180°C, and an injection time of 15 seconds. The following step would be to remove the paraffin wax and stearic acid in the debinding process, where the green parts are soaked in n-heptane in a Memmert water bath for 7 hours at 60°C to obtain the brown part. In the next step, the brown part would then undergo thermal debinding for 60 minutes at 450°C to remove the remaining binder, followed by sintering at a temperature of 1300°C with a dwell time of 2 hours inside a tube furnace under vacuum and under argon-5% hydrogen atmospheres. Figure 1 shows the sintering cycle. The samples in this experiment would be addressed as the 1 vol.% Cu under vacuum (S1), 3 vol.% Cu under vacuum (S2), 1 vol.% Cu under argon-5% hydrogen (S3), and 3 vol.% Cu under argon-5% hydrogen (S4) as presented in Table 1.

Table 1 Sample nomenclature and description

Sample nomenclature	Sample description
S1	SS-3vol.%Ti-1vol.%Cu (Vacuum)
S2	SS-3vol.%Ti-3vol.%Cu (Vacuum)
S3	SS-3vol.%Ti-1vol.%Cu (Ar95%-H25%)
S4	SS-3vol.%Ti-3vol.%Cu (Ar95%-H25%)

RESULTS AND DISCUSSION

Metal Powders and Fabricated Samples

The SEM images of the metal powders are shown in Figure 2, and the green, brown, and sintered parts are shown in Figure 3. The 316L Stainless steel powder and titanium powder are irregular, whereas the powder shape of copper is spherical. The shapes of the particles play a role in the grain boundaries of the alloy. Haferkamp et al. [5] claim that a spherical shape powder indicated greater flowability with lower porosity than other shapes. Moreover, a difference in the particle shapes will affect the grain boundaries of the alloy, which subsequently affects the characteristics of the alloy.

Density, Shrinkage and Mass Loss of The Sintered Samples

The density meter (Model: Mettler Toledo AX205) will be used for the measurement of the density of the samples with reference to the ASTM B962-17 (using archemidis' principle), with the result shown in Table 2. The collected data showed that the relative density of the sintered samples ranges from 84.0% to 89.9%, which is far from the expected 95% usually observed [6]. With such a high level of porosity in the samples, it is expected that the copper oxidised during the sintering

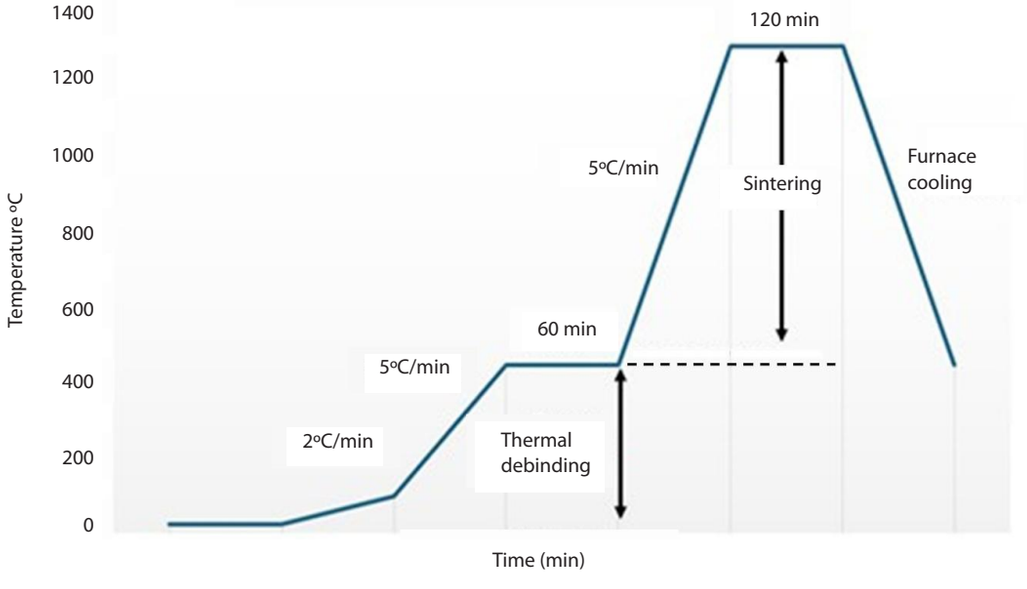

Figure 1 Thermal debinding and sintering cycle

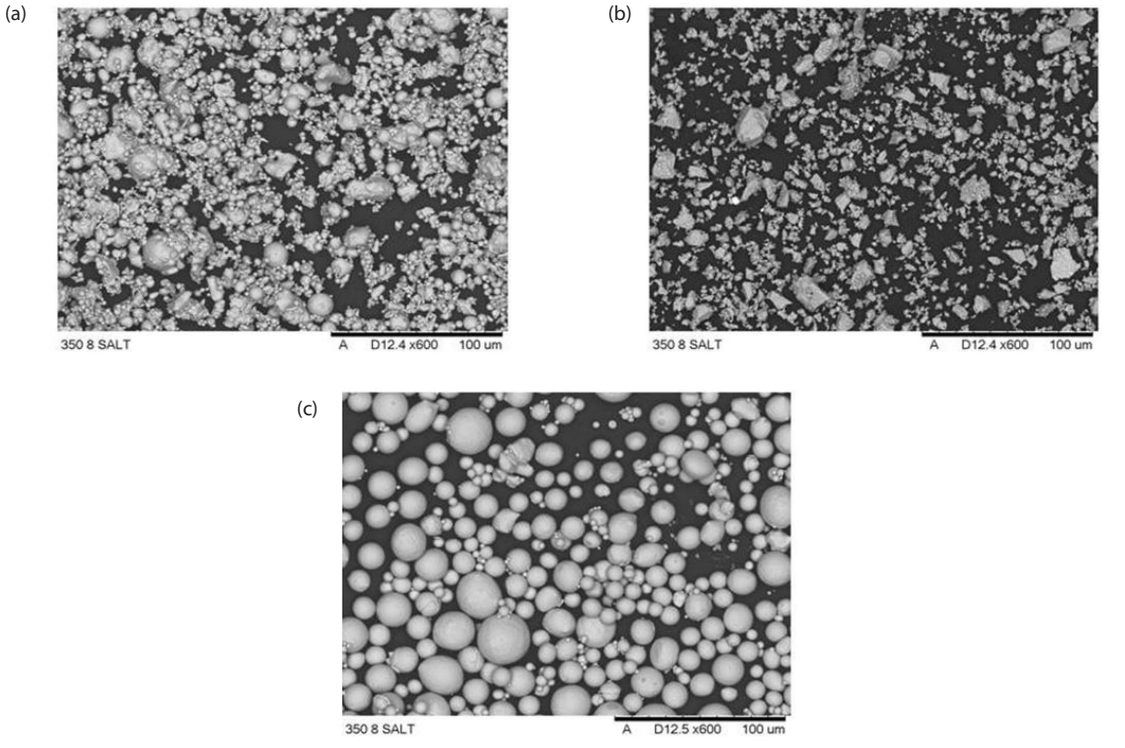

Figure 2 SEM image of (a) 316L Stainless steel powder, (b) Titanium powder, (c) Copper powder

Figure 3 SEM image of (a) Green part, (b) Brown part, (c) Sintered part, (d) Completely oxidised part

phase to form copper oxide, which stops the copper from filling up the pores of the samples. With a high amount of porosity, the mechanical properties such as the tensile strength and hardness of the alloy will be affected since there are fewer particles bonded together. Table 3 shows the mass of the samples in the form of green and sintered parts, including the mass loss. In terms of the mass loss of the samples throughout their fabrication phase, all samples displayed relatively similar mass loss at 20% apart from the S4 sample at 13.8% due to the larger sample thickness. The shrinkages of the samples observed were similar for all samples in the 11.00% to 12.35% range. The equations for sintered density, theoretical density, the shrinkage and mass loss are presented as:

$$\rho_{sintered} = (\rho_{water} - \rho_{air}) \cdot \frac{m_{air}}{m_{air} - m_{water}} + \rho_{air} \quad (1)$$

$$\rho_{theoretical} = \rho_F V_F + \rho_M V_M \quad (2)$$

$$Shrinkage\ (\%) = \left(\frac{L_o - L_f}{L_o} \right) \quad (3)$$

$$Mass\ loss\ (\%) = \left(\frac{m_o - m_f}{m_o} \right) \quad (4)$$

Here, ρ_{water} is the density of the sintered sample in water, and ρ_{air} is the density of the sintered sample in air, whereas m_{air} is the mass of the sintered sample in air and m_{water} is the mass of the sintered sample in water. Here the ρ_F is the density of reinforcement (Cu+Ti) and ρ_M is the sintered density of 316L SS. V_F and V_M is the volume fraction of reinforcement and matrix. L_o and m_o are the lengths and masses of green samples (injection moulded samples), and L_f and m_f are the lengths and masses of the sintered samples.

Tensile Test

The tensile strength, strain and maximum elongation of the samples were obtained through the tensile test. The equipment used to run the test is the universal testing machine, and it is performed based on the ASTM E8M standard with a 0.008 mm/s strain rate under room temperature conditions. The stress-strain curve of all the samples is shown in Figure 4, with the tensile strength at yield and Young's modulus illustrated in Figure 5. The maximum elongation and strain of the samples are shown in Figure 6. From the tensile test, S1 has the highest Young's modulus out of the four samples. The S2 sample is considered an anomaly as it yields low mechanical properties because the fabricated sample is not flat, as illustrated in Figure 7. S3 yields the highest tensile strength, whereas S4 samples have the highest elongation and strain. This aligns with [6] whereby a low density of the samples leads to a reduction in mechanical properties.

Microhardness Test

The microhardness test was carried out to characterise the hardness of the alloy. The microhardness tester (Model: Leco LM247AT) is used with a pyramidal

Table 2 Density of the samples

Sample	Theoretical density (g/cm^3)	Measured sintered density (g/cm^3)	Relative density (%)	Calculated porosity (%)
S1	7.72	6.94	89.90	10.10
S2	7.74	6.92	89.41	10.59
S3	7.72	6.78	87.82	12.18
S4	7.74	6.5	83.98	16.02

Table 3 Mass and shrinkage of the samples

Sample	Mass of green part (g)	Mass of sintered part (g)	Mass loss (g)	Mass loss (%)	Shrinkage (%)
S1	17.5	14.05	3.45	19.72	11.00
S2	17.67	14.05	3.62	20.50	11.53
S3	14.68	11.63	3.05	20.78	12.04
S4	20.16	17.38	2.78	13.79	12.35

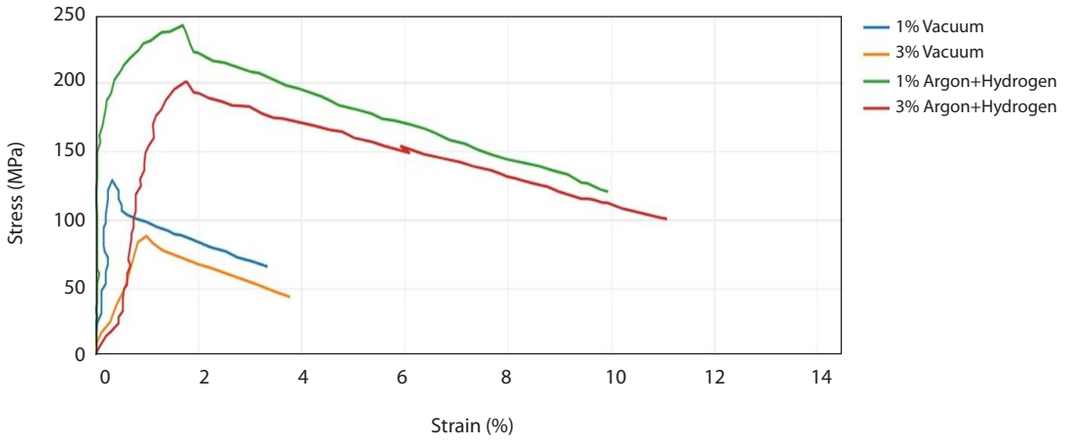

Figure 4 Stress-strain curve for all the samples

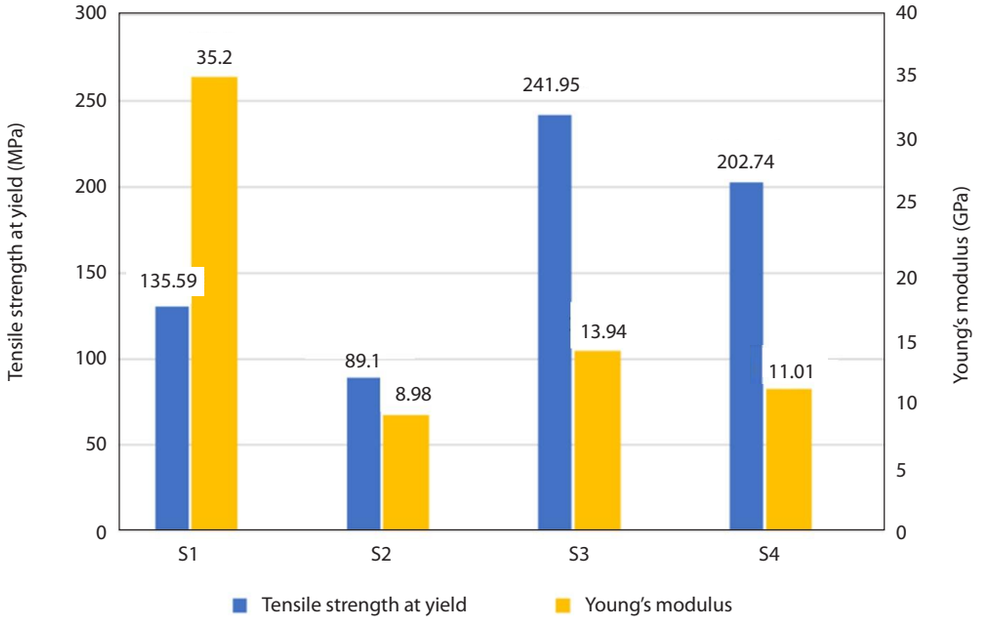

Figure 5 Tensile strength at yield and Young's Modulus for all the samples

shape tip with 1000 gf for 10 seconds. The results of the microhardness value are plotted in Figure 8. Based on the data obtained from the microhardness test, S2 yields the highest value at 131 kgf/mm^2 with high deviation compared to the remaining sample, which exhibits a similar value with minimal deviation for S3 and S4 samples. However, these values obtained were far from the 316L-Ti samples, which exhibit a microhardness in the range of 240 kgf/mm^2 to 270 kgf/mm^2 from the samples of Shahed et al. [6].

Microstructure of The Sintered Samples

The samples were ground with silicon carbide paper with grit paper grades from 120 to 2000. Then, the samples are polished with a polishing paper with Diamond Polishing Paste (6 µm) applied on the polishing paper, followed by another polishing step with the Polycrystalline Diamond Suspension (3 µm) and a third step with the Polycrystalline Diamond Suspension (1 µm). The samples are then electrically etched with 2% nital etchant solution, carried out at 13 V for 3 minutes. After etching, the microstructure analysis is performed. The optical microscope (Model:

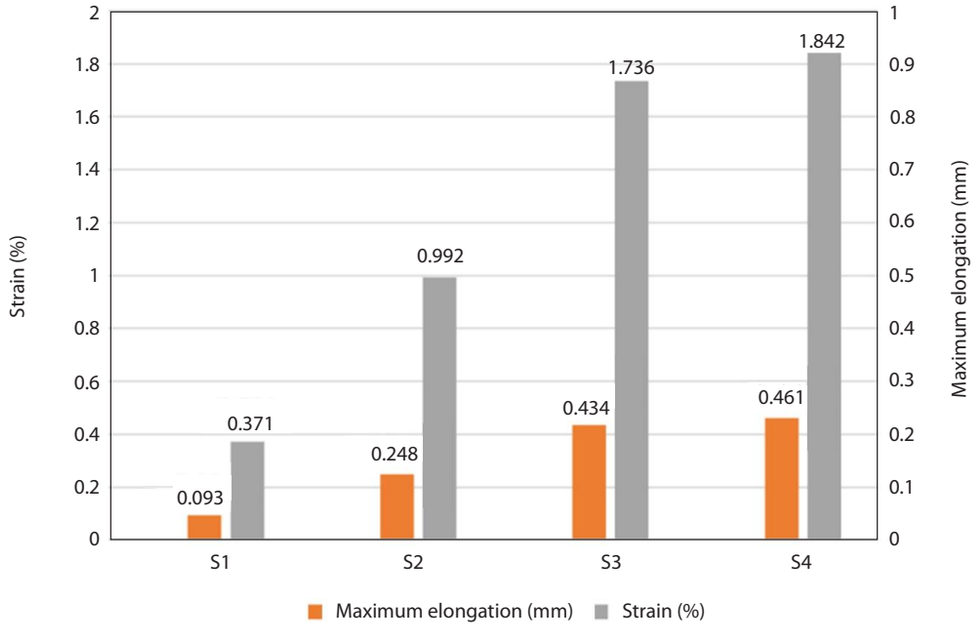

Figure 6 Maximum elongation and strain of all the samples

Figure 7 Uneven sample clipped by the universal tensile machine

Leica DM2700 P) examines the alloy's microstructure with 20x and 50x magnification. The microstructures of the fabricated samples are displayed in Figure 9 for 20x magnification and Figure 10 for 50x magnification.

The microstructure showed that the 1% Cu samples, regardless of sintering conditions, show more refined grain boundaries compared to the 3% Cu samples, which have larger grain boundaries.

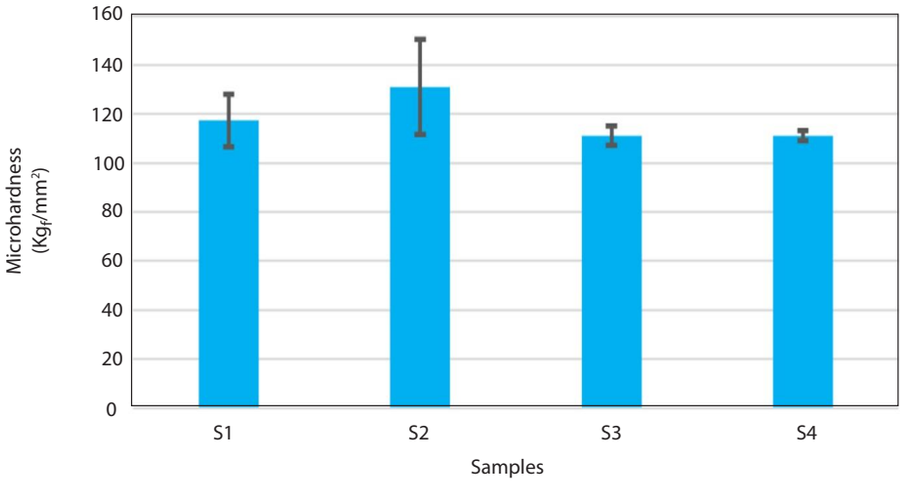

Figure 8 Microhardness of the samples

SEM and EDS Analysis on The Sintered Samples

The SEM images and EDS mapping are illustrated in Figure 11. Samples S3 and S4, which are sintered under argon-hydrogen sintering, show a high amount of pores, which explains the reduction of density. Compared to those samples sintered under a vacuum atmosphere, the grain boundaries of both samples can be observed with minimal pores. The EDS results show that the titanium particle can be observed clearly in all samples. One key observation was that S3 samples suggest the presence of an intermetallic compound from the Fe-Ti phase diagram system.

Fractography Analysis

SEM analysis was conducted on the fractured samples after the tensile test to gain a deeper understanding of the internal topography of the samples (Figure 12). From the EDS results of S1, S3 and S4, certain sections of

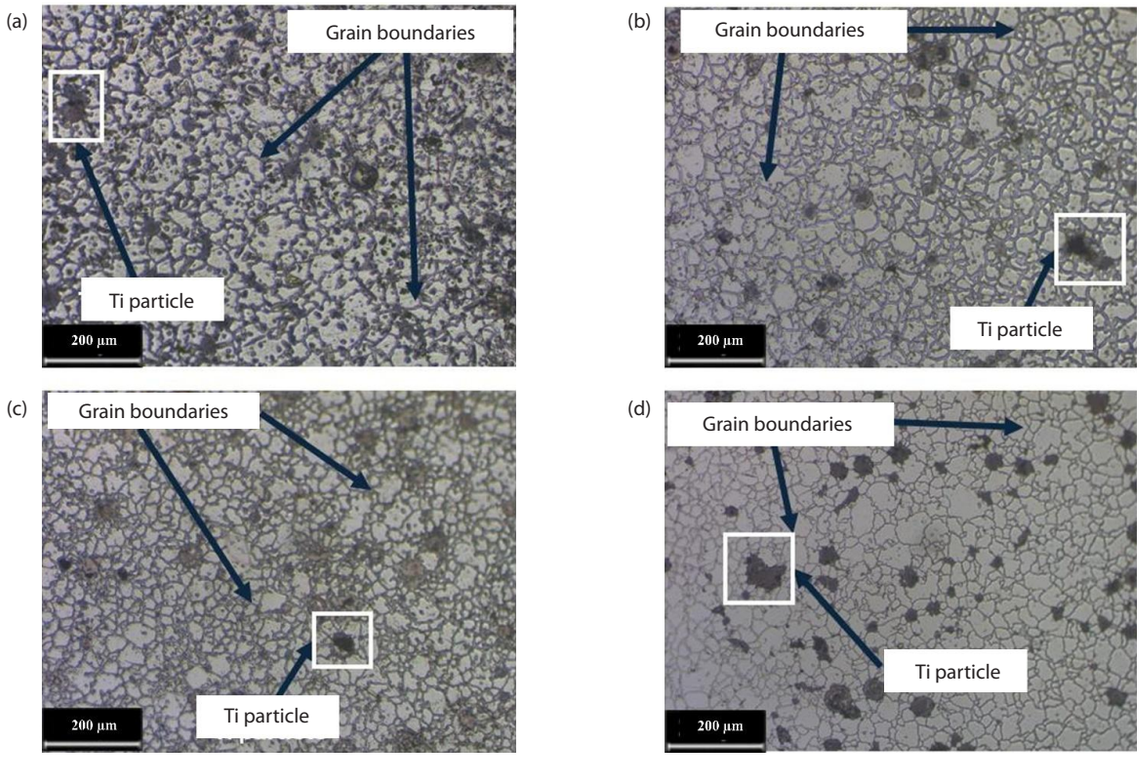

Figure 9 20x magnification of sample (a) S1 (b) S2 (c) S3 (d) S4

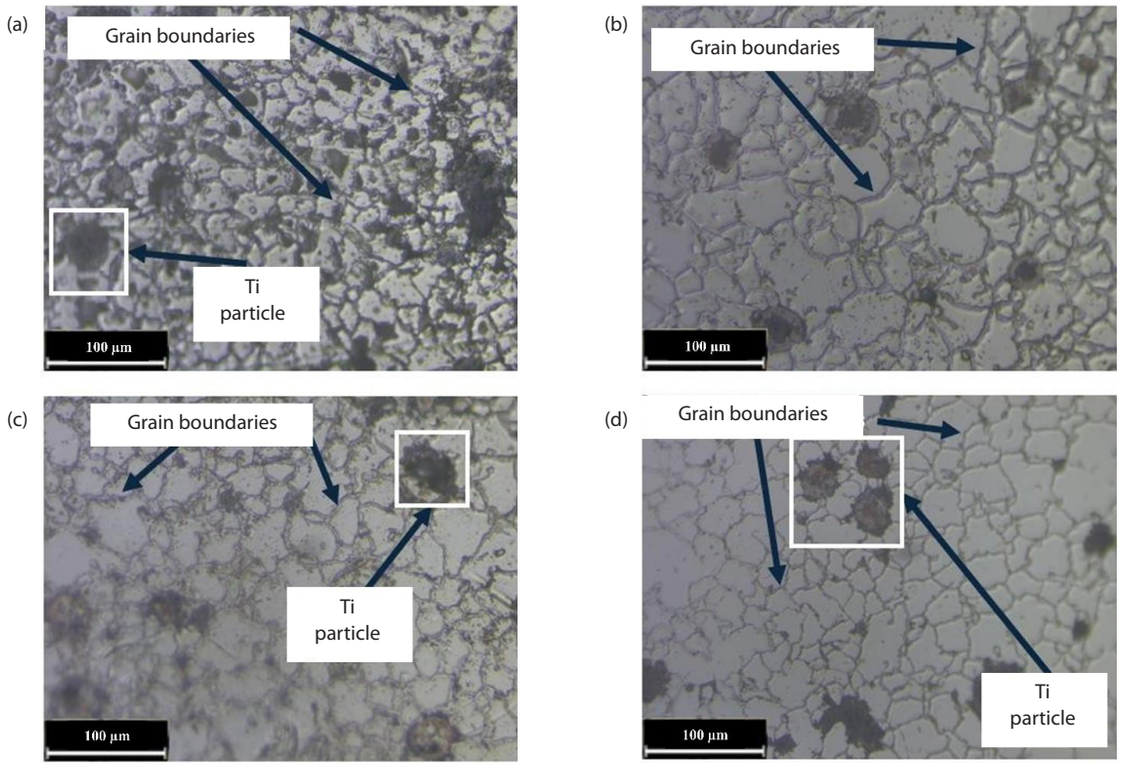

Figure 10 50x magnification of sample (a) S1 (b) S2 (c) S3 (d) S4

the sample cannot be detected by EDS due to uneven surfaces on the samples caused by the fracture during the tensile test.

From the results of the fractured samples, it was found that there is a high amount of oxygen present in all of the samples, indicating that there is a formation of oxides such as titanium oxide and copper oxide. This element was not detected on the polished samples as the grinding and polishing process has removed the oxides. These oxides would then act as a barrier to stop the sintering process, which compromises the pore filling

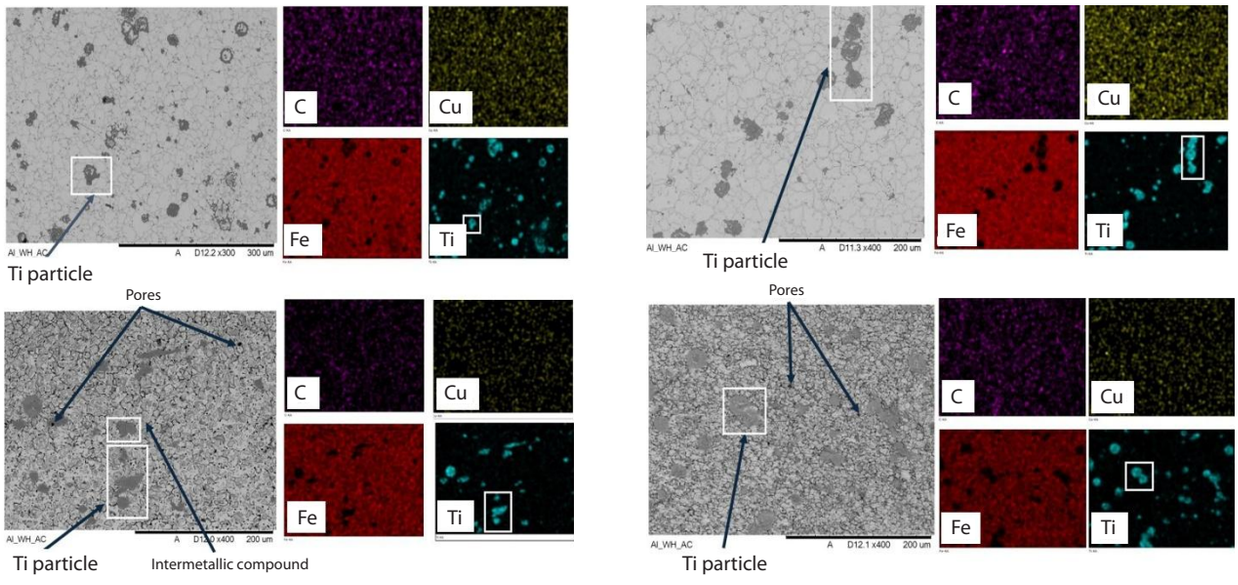

Figure 11 SEM micrograph and EDS mapping of (a) S1, (b) S2, (c) S3, and (d) S4 samples

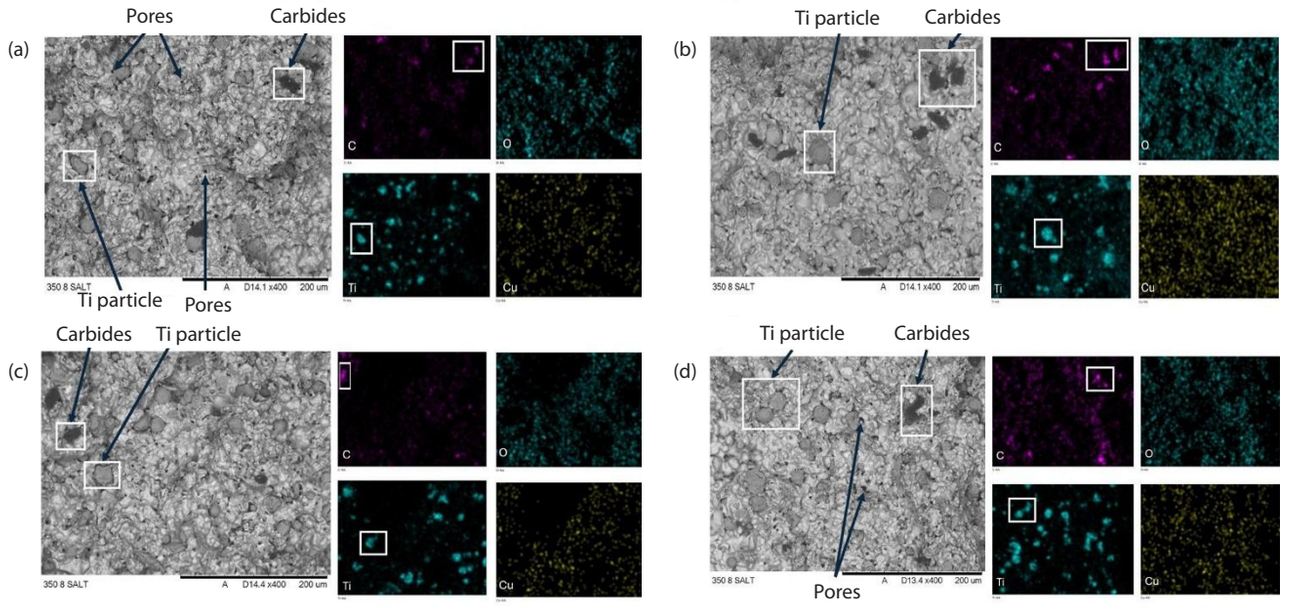

Figure 12 SEM micrograph and EDS mapping of fractured (a) S1, (b) S2, (c) S3, and (d) S4 samples

and thus leaves high amounts of pores on the samples. The observation also shows that the samples are not completely sintered due to the oxidation of copper and titanium formed on the samples, which serves as evidence of the low densification of the samples, consequently affecting their mechanical properties.

In addition, carbon was present in all of the fractured samples, suggesting that carbides were formed. These carbides are possibly formed from either titanium or stainless steel or both. The characteristic of these carbides is that they are brittle, which can justify the brittleness shown by the fabricated samples, especially those sintered in vacuum. Moreover, porosity observed on the samples could also be caused by incomplete thermal debinding, whereby the binders, especially the polypropylene, are not fully removed from the samples, which can heavily affect the properties of the alloy. This, however, can easily be solved by simply increasing the dwell time for thermal debinding.

Discussion on The Sintered Samples

From the variation of the copper, it was discovered that the change in copper content did not affect the physical properties of the alloy, but for the mechanical properties, it was noticed that the tensile strength at yield reduces when the copper content is increased. This was accompanied by a greater elongation, leading to a lower value of Young's modulus. Comparing the mechanical properties between the 316L-Ti from [6] and the 316L-Ti-Cu in this study. For the same titanium content at 3 vol% and sintering temperature of 1300°C, 316L-Ti yields significantly greater mechanical and physical properties than the samples of 316L-Ti-Cu sintered in different environments. Thus, this differs from the findings of Liu et al. [11] and Xi et al. [12], where alloying titanium and stainless steel improved the mechanical properties of the alloy, although the types of metals involved in their research are limited to only two types.

The findings from the two different sintering environments were highly significant. The vacuum atmosphere yields greater overall sintered density relative to those sintered under an argon-hydrogen atmosphere. This is due to the high level of pores observed on the samples, which contributed to the alloy's low density and mechanical properties. This observation is consistent with the findings presented in [6], which indicate that the reduction in strength is a consequence of insufficient densification of the alloy. These findings concerning the sintering atmosphere are validated by Pieczonka et al. [13], whereby the author claims that the oxygen content in argon-hydrogen sintering contains 0.10wt.% more than the samples sintered under vacuum atmosphere, proving that the vacuum atmosphere manages to remove the presence of oxygen more effectively.

Furthermore, Schaffer et al. [14] also argue that vacuum sintering yields better results than those sintered in nitrogen-hydrogen and argon-hydrogen. However, one contradicting observation was that the samples sintered in argon-hydrogen yield significantly higher tensile strength and ductility than those sintered in a vacuum atmosphere. This is aligned with one of the findings of Luo et al. [15], where sintering under argon yields significantly greater ductility. However, the tensile strength obtained was similar to that sintered in vacuum. Therefore, the higher tensile strength factor could be attributed to the possibility of the bonding between the 316L-Ti-Cu, which allows it to endure greater stress despite having a higher density of pores found in those samples.

One consideration that needs to be taken into account is the mechanism of the sintering process. Luo et al. [15] summarised that if the sintering process is conducted other than in vacuum, the gas will be entrapped, causing a high amount of porosity. Besides that, Schaffer et al. [14] claim that a reaction that can consume the atmosphere will reduce gas pressure within the porosity and thus, increase the rate of sintering. If there are gases entrapped within the pores, it will affect the efficacy of the sintering process by reducing the pore filling and consequently, the densification is heavily reduced. This serves as evidence of the high amount of porosity observed on the samples sintered in argon-hydrogen atmosphere. Argon is known for its inert properties, which means liquid copper will not react with argon; this will entrap the gases within the pores, reducing the densification as seen on the samples.

Based on the fundamental understanding of material, crystal structure is vital in determining the characteristics that the material exhibits. For titanium, intermetallic compounds form between iron and titanium, as well as beta-titanium in both variations of copper. Intermetallic compounds such as these are brittle, which could also serve as an explanation for the brittle behaviour exhibited by the samples. For the β-Ti, Shahed et al. [6] summarise that the β-Ti formation will lower the Young's modulus of the alloy. The crystal structure of the iron will be ferrite based on the Fe-Ti system and austenite from the Fe-Cu system. This leads to a mixture of BCC and FCC crystal structures, which aligns with their findings [6], where both ferrite and austenite phases were detected during the XRD analysis.

Another possible factor contributing to the high amount of porosity achieved was that the copper has oxidised to form copper (II) oxide (Cu_2O), which acts as a barrier to stop the particles from bonding and filling up the pores. This is because copper easily oxidises even with a slight presence of oxygen to form Cu2O [16]. In one of the sintering cycles, a leakage was detected on the tube furnace, causing the pressure to drop. This then leads to an increased oxygen level, which allows copper to react with oxygen to form copper oxide on the samples completely, which explains that the colour is black, which is that of Cu2O. Figure 3d illustrates the samples that are completely oxidised.

CONCLUSION

The study concludes that copper significantly influences the properties of 316L-Ti-Cu alloy, with 316L-Ti exhibiting superior mechanical and physical performance compared to 316L-Ti-Cu, though copper's impact on physical properties was negligible in both sintering atmospheres. Sintering environment played a critical role, as samples sintered in argon-5% hydrogen showed higher yield tensile strength but lower Young's modulus, indicating higher ductility compared to vacuum-sintered samples. However, sintering in argon-hydrogen atmosphere led to excessive porosity due to copper oxide formation, reducing sintered density, while vacuum sintering yielded denser samples with better mechanical properties. Optimising sintering temperature can be studied in future studies to further enhance alloy performance. Additionally, the sintering atmosphere and mechanisms require deeper investigation to fully optimise the alloy's properties. Future studies should also explore the alloy's antibacterial potential, leveraging copper's ability to release ions that combat implant-related infections and its corrosion behaviour to assess ion release and implant degradation for compatibility evaluation. These findings highlight the need for further research to refine processing parameters and evaluate biomedical applicability.

ACKNOWLEDGMENT

The authors would like to thank the Department of Mechanical Engineering, Universiti Teknologi PETRONAS (UTP), Malaysia, for supporting this research, which is gratefully acknowledged.

REFERENCES

[1] A. Sumayli, "Recent trends on bioimplant materials: A review," *Materials Today: Proceedings*, pp. 2726-2731, 2021, doi: 10.1016/j.matpr.2021.02.395.

[2] D. Sivaraj and K. Vijayalakshmi, "Novel synthesis of bioactive hydroxyapatite/f-multiwalled carbon nanotube composite coating on 316L SS implant for substantial corrosion resistance and antibacterial activity," *Journal of Alloys and Compounds,* vol. 777, pp. 1340-1346, 2019, doi: 10.1016/j.jallcom.2018.10.341.

[3] A. Awasthi, K.K. Saxena, and R.K. Dwivedi, "An investigation on classification and characterisation of bio materials and additive manufacturing techniques for bioimplants," *Materials Today: Proceedings,* vol. 44, pp. 2061-2068, 2021, doi: 10.1016/j.matpr.2020.12.176.

[4] C.P. Priyanka, K. Keerthi Krishnan, U. Sudeep, and K. K. Ramachandran, "Osteogenic and antibacterial properties of TiN-Ag coated Ti-6Al-4V bioimplants with polished and laser textured surface topography," *Surface and Coatings Technology,* vol. 474, 2023, doi: 10.1016/j.surfcoat.2023.130058.

[5] L. Haferkamp, L. Haudenschild, A. Spierings, K. Wegener, K. Riener, S. Ziegelmeier, and G.J. Leichtfried, "The Influence of Particle Shape, Powder Flowability, and Powder Layer Density on Part Density in Laser Powder Bed Fusion," *Metals,* vol. 11, no. 3, 2021, doi: 10.3390/met11030418.

[6] C.A. Shahed, F. Ahmad, E. Gunister, and K. Altaf, "Microstructure and mechanical performance of low-cost biomedical- grade Titanium-316L alloy," *Journal of Materials Research and Technology,* vol. 27, pp. 8008-8022, 2023, doi: 10.1016/j.jmrt.2023.11.252.

[7] M. Bao, Y. Liu, X. Wang, L. Yang, S. Li, J. Ren, G. Qin, and E. Zhang, "Optimisation of mechanical properties, biocorrosion properties and antibacterial properties of wrought Ti-3Cu alloy by heat treatment," *Bioact Mater,* vol. 3, no. 1, pp. 28-38, Mar 2018, doi: 10.1016/j.bioactmat.2018.01.004.

[8] A. Jacobs, G. Renaudin, C. Forestier, J. M. Nedelec, and S. Descamps, "Biological properties of copper-doped biomaterials for orthopedic applications: A review of antibacterial, angiogenic and osteogenic aspects," *Acta Biomater,* vol. 117, pp. 21-39, Nov 2020, doi: 10.1016/j.actbio.2020.09.044.

[9] S. Jin, L. Ren, and K. Yang, "Bio-Functional Cu Containing Biomaterials: a New Way to Enhance Bio-Adaption of Biomaterials," *Journal of Materials Science & Technology,* vol. 32, no. 9, pp. 835-839, 2016, doi: 10.1016/j.jmst.2016.06.022.

[10] S.J. Gobbi, V.J. Gobbi, and Y. Rocha, "Requirements for Selection or Development of a Biomaterial," vol. 14, no. 3, 2019, doi: 10.26717/BJSTR.2019.14.002554.

[11] J. Liu, F. Li, C. Liu, H. Wang, B. Ren, K. Yang, and E. Zhang, "Effect of Cu content on the antibacterial activity of titanium-copper sintered alloys," *Mater Sci Eng C Mater Biol Appl,* vol. 35, pp. 392-400, Feb 1 2014, doi: 10.1016/j.msec.2013.11.028.

[12] T. Xi, M.B. Shahzad, D. Xu, Z. Sun, J. Zhao, C. Yang, M. Qi, and K. Yang, "Effect of copper addition on mechanical properties, corrosion resistance and antibacterial property of 316L stainless steel," *Mater Sci Eng C Mater Biol Appl,* vol. 71, pp. 1079-1085, Feb 1 2017, doi: 10.1016/j.msec.2016.11.022.

[13] T. Pieczonka, T. Schubert, S. Baunack, and B. Kieback, "Sintering_Behaviour_of_Aluminium_in_Different_Atmo.pdf," *In Proceedings of the Conference 'Sintering'0,* pp. 331-334, 2005.

[14] G. Schaffer, B. Hall, S. Bonner, S. Huo, and T. Sercombe, "The effect of the atmosphere and the role of pore filling on the sintering of aluminium," *Acta Materialia,* 2005, doi: 10.1016/j.actamat.2005.08.032.

[15] S.D. Luo, B. Liu, J. Tian, and M. Qian, "Sintering of titanium in argon and vacuum: Pore evolution and mechanical properties," *International Journal of Refractory Metals and Hard Materials,* vol. 90, 2020, doi: 10.1016/j.ijrmhm.2020.105226.

[16] M. Nishimoto, R. Tokura, M. T. Nguyen, and T. Yonezawa, "Copper Materials for Low Temperature Sintering," *Materials Transactions,* vol. 63, no. 5, pp. 663-675, 2022, doi: 10.2320/matertrans.MT-N2021004.